New tellurite glasses and crystalline phases in the Bi_2O_3–CaO–TeO_2 system: Synthesis and characterization

Abdeslam Chagraoui*, Abdelmjid Tairi, Kaltoum Ajebli, Hanane Bensaid, Abdenajib Moussaoui

Laboratoire de Chimie Analytique et Physico-chimie des Matériaux, Département de Chimie, Faculté des Sciences Ben M'sik, Université HassanII-Mohammedia Casablanca, Morocco

ARTICLE INFO

ABSTRACT

Tellurite glasses containing calcium and bismuth oxides have been prepared at 800 °C and investigated by X-ray diffraction, DSC, IR and Raman spectroscopy. The crystalline phases of glasses in TeO_2–CaO revealed γTeO_2 phase which transforms into the stable αTeO_2 phase up to 500 °C. IR and Raman studies show the transition of TeO_4, TeO_{3+1} and TeO_3 units with increasing CaO content. The value of refractive index and density of glasses have been measured. The investigation in the system using XRD reveals new phases.

© 2010 Published by Elsevier B.V.

1. Introduction

Tellurite-based glasses are of technological interest because of their low melting temperature, high refractive index, good transmission in the infrared region and optical non-linearity. They are also not hygroscopic and have superior physical properties such as high dielectric constant and low melting point (800 °C) [1–4]. The origin of the extraordinary non-linear optical properties of TeO_2-based glasses is attributed to high hyperpolarizability of a lone electron pair related to the 5s orbital of tellurium atom [5,6]. TeO_2 dioxide is four-coordinate; although this oxide itself is only a conditional glass former; addition of heavy metal oxide (PbO, WO_3, Nb_2O_5, ZnO, BaO, etc.) rises to ranges of excellent glass formation and in fact enhanced stability against devitrification [7–12]. Tellurite glasses are also considered as one of the best hosts for doping with rare earth elements. They are good candidates for practical laser applications [13,14].

The present paper reports a preliminary investigation of new tellurite glasses and crystalline phases in Bi_2O_3–CaO–TeO_2 system. Elaboration process, thermal properties infrared (IR) and Raman studies in comparison to analogous crystalline phases will be described successively.

2. Experimental

The amorphous and crystalline samples were prepared using high purity commercial materials Bi_2O_3, TeO_2 and $CaCO_3$ of analytical grade (Aldrich 99.9%). The batches of suitable proportions of starting products were mixed in an agate mortar and then melted in air in porcelain crucible at 800 °C (30 min) for vitreous phases and at 750–850 °C (48 h) for crystalline phases. All of them are quenched to room temperature and identified by X-ray diffraction (XRD) using a Bruker D8 Advance diffractometer (Cu Kα radiation). T_g (glass temperature) and T_c (crystallization temperature) were determined by Differential Scanning Calorimetry (DSC) Netsch 2000 PC type from powder samples glasses for about 8 mg in aluminum pans. A heating rate of 10 °C/min was used in the 30–600 °C range. Infrared absorption measurements between 2000 and 400 cm^{-1} were made for powder specimens dispersed in a pressed KBr disk. The Raman spectra were recorded with an imaging spectrometer (HoloSpec f/1.8i, Kaiser Optical Systems) equipped with a holographic transmission grating and thermoelectrically cooled two-dimensional multichannel CCD detector (Newton, Andor Technology, 1600×400 pixels, -60 °C). An argon laser was used for the excitation and the 514.5 nm wavelength radiation was chosen.

The refractive index of some compositions was determined with an optical microscope NIKON model 104 by successive focusing on the two parallel faces of polished samples. The densities of samples were determined on blocks of glasses by Archimede's method using diethylorthophtalat as liquid.

3. Results and discussion

A wide range glass system based on the Bi_2O_3–TeO_2–CaO was successfully prepared at 800 °C. Glass formation region is obviously dependent on the temperature, so this temperature has been chosen to have a homogenous reagent on one hand, and to avoid volatization of TeO_2 at high temperature (T_{TeO_2} Melting = 732 °C)
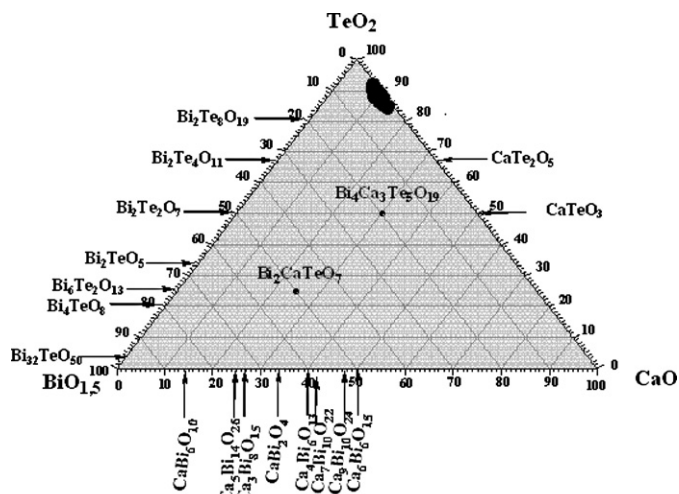
Fig. 1. Phase diagram of Bi_2O_3–CaO–TeO_2 system with new phases: Bi_2CaTeO_7 and $Bi_4Ca_3Te_5O_{19}$.

on the other hand (Fig. 1). The color of the glass changes slightly from dark yellow to yellow with increasing CaO and Bi_2O_3 concentrations.

In pseudo-binary CaO–TeO_2, the vitreous compositions are 5–15 mol% CaO content (Fig. 1). In comparison with pseudo-binary BaO–TeO_2 [15] and SrO–TeO_2 [16] studies previously this field is narrow. It seems that the vitreous field is closely related to the size of modifying oxide ($rBa^{2+} = 1.34\,\text{Å} > rSr^{2+} = 1.16\,\text{Å} > rCa^{2+} = 1.00\,\text{Å}$ [17]).

The curves (DSC) exhibit endothermic effect due to glass transition (T_g); the value of T_g is evaluated from the point of reflection of this change. At still higher temperatures three exothermic peaks Tc are observed corresponding to crystalline phases. Figs. 2 and 3 show the dependence of characteristic temperature, glass transition, the first crystallization (Tc_1), the second (Tc_2) and the third crystallization (Tc_3) on CaO content. The values of T_g, Tc_1, Tc_2 and Tc_3 are presented (Fig. 2 and Table 1). The appearance of single peak (all glasses) due to the glass transition temperature indicates the homogeneity of the glasses prepared. With the increase in the concentration of CaO in the glass matrix, the T_g increases and the difference ($Tc - T_g$) (about 20–50 °C) implies a thermal stability of glasses. In a study of alkali tellurite glasses, Inoue and Nukui [18] showed that the temperature of the glass transition decreases with increasing amount of Li, Na or K compounds. The dependence of CaO content shows a different tendency, especially of glass transition compared with the alkali tellurite glasses. The alkali atoms easily move in the glass structure. However, Ca ions move with greater difficulty in the glass, because the Ca atom is restrained by relatively strong bands to every coordinate oxygen. The light change of the temperature of crystallization of a vitreous composition to another is due to the kinetic phenomenon. Based on XRD and DSC analysis for glassy samples 5–15 mol% CaO (see Fig. 4) a first peak of crystallization corresponds to the αTeO_2 and the γTeO_2 polymorphic at 380–390 °C range.
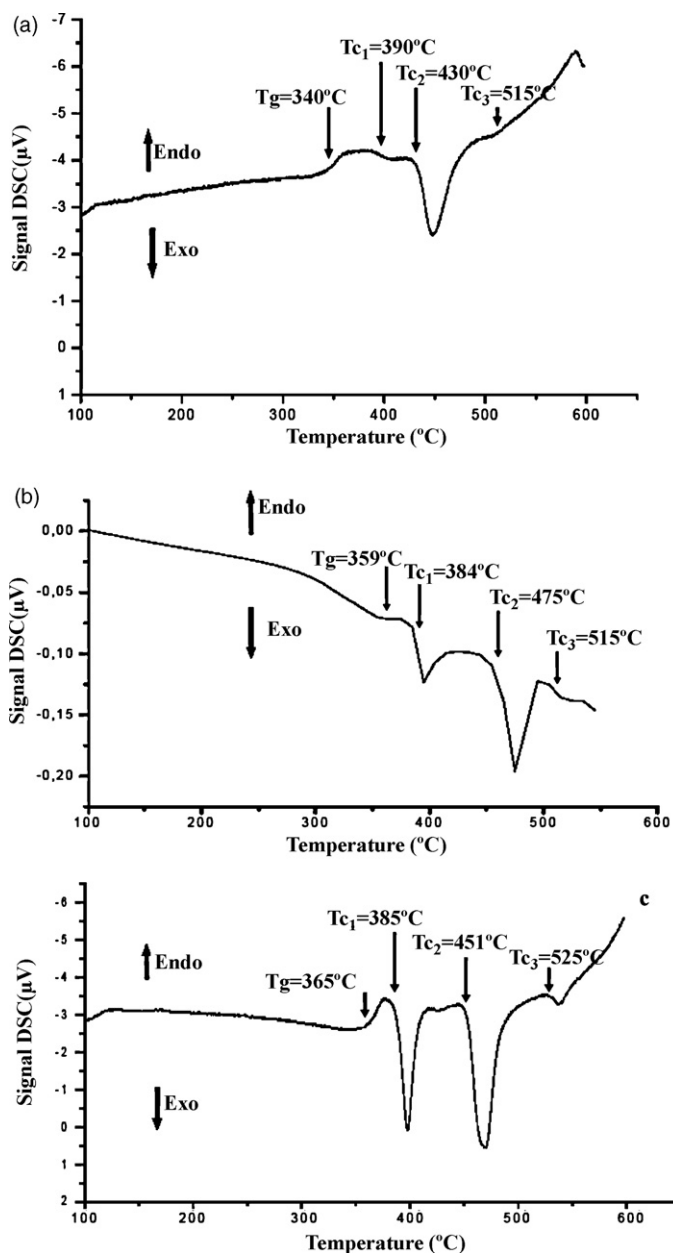

Fig. 2. DSC curves of glassy samples (5 mol% CaO (a), 10 mol% CaO (b), 15 mol% CaO (c)) obtained in CaO–TeO_2 pseudo-binary.
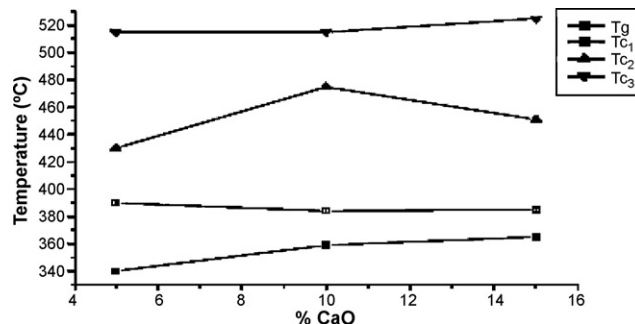
Fig. 3. Evolution of glass transitions (T_g) and crystallizations (Tc) with composition.

Table 1

Characteristics (T_g, Tc) and difference ($Tc_1 - T_g$) of some glasses in the CaO–TeO_2–Bi_2O_3 system.

mol% $BiO_{1.5}$	mol% TeO_2	mol% CaO	T_g (°C)	Tc_1 (°C)	Tc_2 (°C)	Tc_3 (°C)	$Tc_1 - T_g$
0	95	5	340	390	430	515	50
0	90	10	359	384	475	515	25
0	85	15	365	385	451	525	20

Fig. 4. XRD patterns heat-treated at 420 °C, 500 °C and 550 °C of 90 mol% TeO$_2$ in pseudo-binary TeO$_2$–CaO.

Table 2
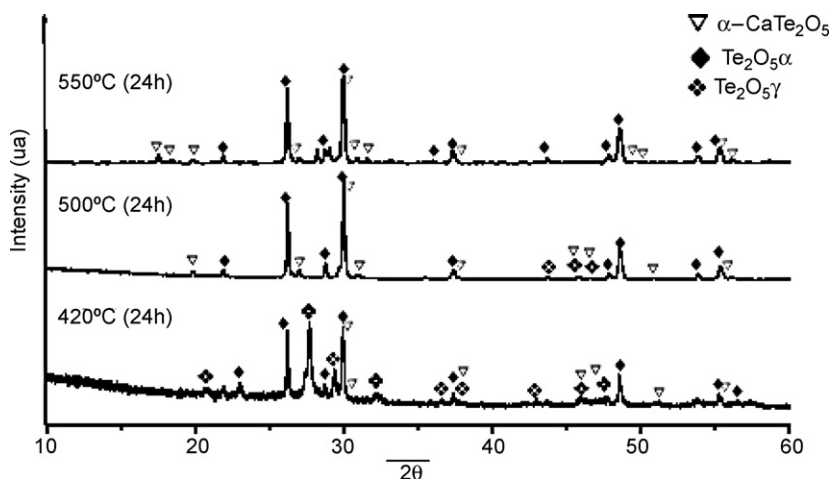Some characteristics physics and phases appearing after annealed of some glasses in the Bi$_2$O$_3$–CaO–TeO$_2$ system.

mol% CaO	mol% TeO$_2$	Refractive index, n (±0.02)	Density (±0.03)	Molar volume (cm^3/mol) (±0.02)	Phases after crystallization
5	95	2.13	5.44	28.39	TeO$_2$(α), TeO$_2$(γ), αCaTe$_2$O$_5$
10	90	2.14	5.32	28.054	TeO$_2$(α), TeO$_2$(γ), αCaTe$_2$O$_5$
15	85	2.15	5.29	27.235	TeO$_2$(α), TeO$_2$(γ), αCaTe$_2$O$_5$

This phenomena is also observed in the system as TeO$_2$–WO$_3$ [8], Nb$_2$O$_5$–TeO$_2$ [8,11], TeO$_2$–ZnO [12,15] and TeO$_2$–SrO [16]. The second crystallization ranging 430–475 °C belongs to αCaTe$_2$O$_5$ phase. The last peak with weak intensity is attributed to the total transformation of γTeO$_2$ metastable polymorph into the stable αTeO$_2$ one. The X-ray diffraction peaks of γTeO$_2$ phase begin to decrease up to 500 °C.

The glasses, when treated at different temperatures (24 h) below their melting temperature, crystallize into the ternary system phases confirm the phases that are crystallizing near the exothermic (Fig. 1).

3.1. Refractive index

Refractive index is one of the most important properties in optical glasses. Therefore, a large number of researchers have carried out investigations to ascertain the relation between refractive index and glass composition. The values obtained in the Bi$_2$O$_3$–CaO–TeO$_2$ system are much higher than that obtained with SiO$_2$ based glass (1.5) (Table 2).

3.2. Density

The density of the specimens was measured using Archimede's principle using orthophtalate as the immersion liquid ($d_{\text{orthophtalate}} = 1.11437$ at 25 °C). A glass disc was weighted in air (W_{air}) and immersed in orthophtalate and reweighted ($W_{\text{orthophtalate}}$). The relative density is given by the following relation [19]:

$$d = d_{\text{orthophtalate}} \frac{W_{\text{air}}}{W_{\text{orthophtalate}}}$$

Variations in the density and molar volume V_m with the composition of prepared binary tellurite glasses are reported in Table 2. In the TeO$_2$–CaO system the glass density and molar volume decrease with the augmentation of CaO/TeO$_2$.

From the result, it can be seen that values of molar volume and density of the glasses change linearly with the addition of CaO in relation and are derived obviously due to the difference of Te and Ca atoms weights.

4. Spectroscopy studies

4.1. IR study

The bands in the IR spectrum of crystalline TeO$_2$ are assigned according to C$_{2v}$ point group symmetry in the following manner:

$$\nu^s = 780 \, \text{cm}^{-1}; \quad \nu^s_{a\,\text{TeOeq}} = 714 \, \text{cm}^{-1};$$

$$\nu^{as} = 675 \, \text{cm}^{-1}; \quad \nu^s = 635 \, \text{cm}^{-1}$$

In the pure TeO$_2$ glass the ν^s band at 635 cm^{-1} increases markedly instated of $\nu^{as}_{\text{TeOax}} = 675$ cm^{-1} and becomes a determining one. The rise of ν_{ax}^s intensity is the result of decrease in the symmetry of the polyhedra in the glass network [20–22] (Fig. 5).

IR spectra of tellurite built up by TeO$_3$ polyhedra with equal lengths of the Te–O show four normal vibrations. Two of them ν(A1)
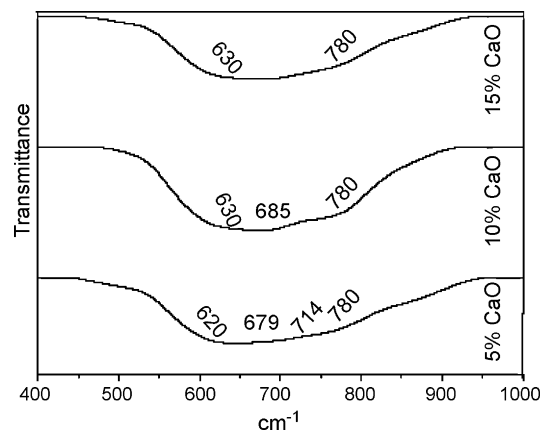

Fig. 5. IR transmission spectra of glasses and crystalline phases of the CaO–TeO$_2$ system.
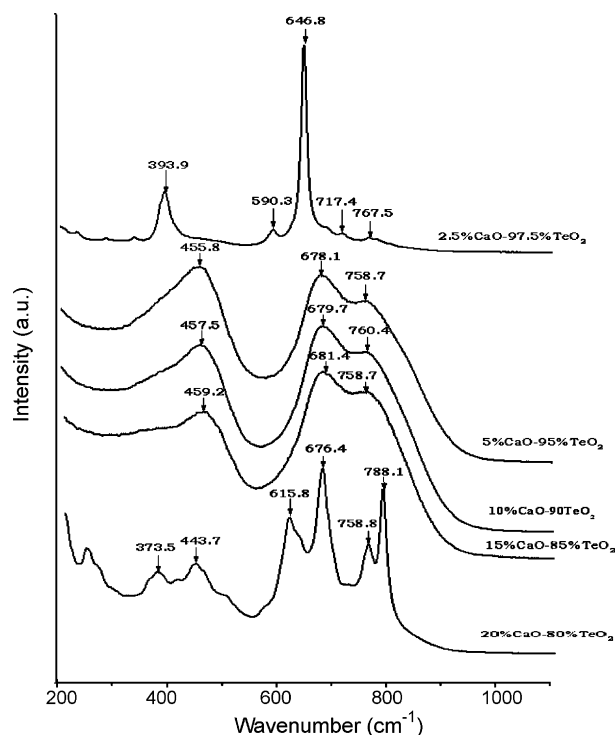
Fig. 6. Raman spectra of glasses and crystalline phases of the CaO–TeO$_2$ system.

and ν(E) correspond to the symmetric (ν^s) and degenerate (ν^d). The polyhedra are assigned to the point group C_{3v} [23,24].

The infrared transmission spectrum of glasses in CaO–TeO$_2$ system (Fig. 6) exhibits vibrational bands in the range 600–800 cm^{-1}. This region may also consist of bands due to anti-symmetrical and symmetrical vibrations of TeO$_2$. For (0–5% CaO content) an intense band is observed nearly at 630 cm^{-1} when compared with crystal (TeO$_2$). It characterizes the presence of non-symmetrical TeO$_4$ groups which give an indication that tellurium does not change its coordination number four in this range of compositions. This band 630 cm^{-1} is attributed to the symmetric vibrations in Oax–Te–Oax groups into TeO$_4$ polyhedra. It is progressively broadening and moving towards the higher energy with CaO content, which is the characteristic of more distortions of TeO$_4$ polyhedra. The second band (shoulder) (nearly observed at 780 cm^{-1}) was attributed to asymmetrical vibrations of TeO$_4$ structural units (Oeq–Te–Oeq). The presence of mainly TeO$_{3+1}$ and TeO$_3$ entities is the signature of breaking off in the tellurite matrix glass network due to a large proportion of added calcium oxide.

The two modes observed nearly at 780 and 630 cm^{-1} can be assigned as the frequency shifts from ν_1(A1) = ν_s(TeO$_4$)$_{eq}$ = 780 cm^{-1} and ν_2(A1) = 650 cm^{-1} with the formation of TeO$_3$ units. The downward shift of the ν_s(TeO$_4$)$_{eq}$ and ν_s(TeO$_4$)$_{ax}$ modes in the spectra of the binary TeO$_2$–MO (or M$_2$O) systems have been reported in the literature [20–23]. According to Dimitrova-Pankova et al. [20] TeO$_{3+1}$ structural units are formed in binary tellurite glasses containing monovalent or bivalent cations as network modifiers. For 10 mol% CaO we observe three bands (630–685–780 cm^{-1}). With increasing modifier content, the deformation of the TeO$_4$ polyhedra became greater, and the symmetry of the TeO$_4$ group decreases. As a result, the mode at 620 cm^{-1} is shifted towards lower frequencies.

4.2. Raman spectra of calcium tellurite glasses

The Raman spectra of xCaO, (100 − x) TeO$_2$ (2.5 ≤ x ≤ 20 mol% fraction) glasses and crystalline phases are shown in Fig. 6. For

Table 3
Indexing of XRD reflections of Bi$_4$Te$_5$Ca$_3$O$_{19}$ phase.

h k l	d_{obs}	d_{calc}	I/I_0
2 0 0	4.587	4.595	22
1 1 1	3.841	3.844	11
0 1 2	3.202	3.202	85
2 1 1	3.059	3.059	100
2 0 2	2.857	2.857	16
3 0 1	2.747	2.746	19
0 0 3	2.710	2.710	22
3 0 $\bar{2}$	2.626	2.625	9
3 2 0	1.982	1.981	10
3 2 $\bar{1}$	1.966	1.966	11
1 0 4	1.926	1.929	8
3 0 3	1.906	1.905	9
4 0 $\bar{3}$	1.881	1.884	6
5 0 $\bar{1}$	1.853	1.848	8
3 1 $\bar{4}$	1.709	1.710	9
1 3 1	1.663	1.653	8
4 0 3	1.643	1.645	7
0 0 5	1.624	1.626	6
2 0 5	1.602	1.603	9
2 3 $\bar{2}$	1.531	1.531	5

5 ≤ x ≤ 15 mol% fraction, spectra obtained from different spots are identical indicating high homogeneity of glasses. Each spectrum was deconvoluted and the Raman bands were assigned based on the literature data [24,25]. The most prominent band at 680–682 cm^{-1} in the spectrum of pure glass is related to the combined vibrations of asymmetric stretching of Te–eqOax–Te bands and symmetric stretching of TeO$_4$ trigonal bipyramid (tbps) [24]. With addition of CaO up to 15 mol% fraction, intensity of these band decreases, while band at 760–762 cm^{-1} attributed to stretching vibrations of non-bridging Te–O– bands in TeO$_3$ trigonal pyramid tps [25] grows in intensity. The wide band at 454–460 cm^{-1} which decreases slightly with increasing CaO content is assigned to the symmetric bending vibration of TeO$_4$ tbps and at the same time symmetric stretching vibration of Te–eqOax–Te linkages which are formed by vertex sharing TeO$_4$ tbps. With the addition of CaO (20 mol%), the intensity of this band decreases, while bands at 760 and 787 cm^{-1} were attributed to stretching vibrations of non-bridging Te–O– bands in TeO$_3$ (tps) grow in intensity. The new band at above 377 cm^{-1} (slightly visible of composition CaO 15 mol%) is assigned to a bending vibration of TeO$_3$ tp having two or three non-bridge oxygen (NBO) atoms. Therefore, the peaks at 445, 616, and 676 cm^{-1} were assigned to TeO$_4$, while the band localized at 760 cm^{-1} is attributed to TeO$_{3+1}$ group [26,27]. The bands of Raman spectrum for 2.5 and 20 mol% compositions of CaO and for fine and confirm as a results acquired by diffraction X for which is excluded from vitreous domain. The Raman spectra of 2.5 mol% CaO is similar to crystalline phase TeO$_2$(α) and for which it is noted two strong peaks at about 392 and 647 cm^{-1}. These peaks are attributed to a TeO$_4$ tbps structural unit in crystalline state [26].

4.3. Crystalline phases

A solid state investigation of the Bi$_2$O$_3$–CaO–TeO$_2$ system allowed synthesis of new phases Bi$_2$CaTeO$_7$ and Bi$_4$Ca$_3$Te$_5$O$_{19}$ which have been obtained at 750–850 °C in air for (48 h) and characterized by XRD. The X-ray powder pattern of Bi$_4$Ca$_3$Te$_5$O$_{19}$ phase was indexed (Table 3) on the basis of monoclinic unit cell parameters: a = 9.278(4) Å, b = 5.196(3) Å, c = 8.208(4) Å, and β = 97.86 (4)° using 10 reflections by the DICVOL program [28]. The observed reflections were indexed and the figure of merit was M(10) = 32.7. The existence conditions of observed reflections lead to possible space groups P$_C$, P$_{2/C}$ or Pm. No significant change in weight was observed, result implies no oxidation of Te^{IV} had occurred and that the formula proposed was correct. It seems the important con-

Table 4
Indexing of XRD reflections of Bi_2TeCaO_7 phase.

h k l	d_{obs}	d_{calc}	I/I_0
0 1 2	4.76	4.81	7
1 1 2	4.36	4.39	5
0 0 3	3.56	3.586	2
2 2 2	3.09	3.10	3
0 2 3	2.97	2.98	100
0 0 4	2.68	2.69	4
2 2 3	2.596	2.609	51
0 3 3	2.522	2.535	3
0 2 4	2.391	2.394	8
1 2 4	2.337	2.336	5
2 3 3	2.283	2.283	6
1 3 4	2.101	2.110	4
1 1 5	2.062	2.071	36
2 3 4	1.990	1.998	3
1 2 5	1.956	1.964	4
0 4 4	1.894	1.902	3
0 1 6	1.762	1.769	4
1 1 6	1.740	1.745	42
0 4 5	1.674	1.680	9
1 4 5	1.656	1.660	4
2 2 6	1.617	1.622	3
0 3 6	1.599	1.604	14

tent of CaO and Bi_2O_3 avoid the oxidation of tellurium tetravalent into tellurium hexavalent. This result is comparable with previous phases such as $Bi_4Te_5Sr_3O_{19}$ [29], $Bi_4Te_5Zn_3O_{19}$ [10] and $Bi_2Te_3W_3O_{16}$ [30]. Bi_2CaTeO_7 isotype Bi_2SrTeO_7 [31] was indexed (Table 4) on the basis of cubic unit cell parameter: $a = 10.7575(1)$ Å with space group Pa$\bar{3}$. The tellurium in this phase is hexavalent. It appears that the small quantity of calcium oxide implies the oxidation in air of TeO_2 in TeO_3 and gives Bi_2CaTeO_7 phase, which is situated in the TeO_3–Bi_2O_3–CaO. The structure determination phase and its relationship with fluorite type will be published.

5. Conclusions

A stable glass has been synthesized in Bi_2O_3–CaO–TeO_2 system at 800 °C. The vitreous crystallization of the samples rich of TeO_2 occurs for the γTeO_2 and αTeO_2 polymorphs. The γTeO_2 variety transforms complete to αTeO_2 up 500 °C. Some physical properties of the glass have been measured. The high linear refractive index of glasses (≈ 2.14) indicates a high optical non-linearity, so they are promising materials for optical communication system. The densities and molar volume of the glasses decrease in CaO content. The characteristic temperatures (glass transition and crystallization temperatures) have been determined. The influence of a gradual addition of the modifier oxides on the coordination geometry of tellurium atoms has been elucidated. Based on IR absorption curves and the Raman spectra of glasses show systematic changes in structural units, from TeO_4 trigonal bipyramid (tbps) to TeO_3 trigonal pyramid (tps) via $[TeO_{3+1}]$ entities with increasing CaO content in glass. A solid state investigation by X-ray of the system allowed synthesis of stable new compounds Bi_2CaTeO_7 and $Bi_4Ca_3Te_5O_{19}$. They derived from the fluorite subcell, which was distorted to monoclinic symmetry for $Bi_4Ca_3Te_5O_{19}$.

References

[1] R. El-Mallawany, J. Appl. Phys. 72 (1992) 1774–1777.
[2] S.H. Kim, T. Yoko, S. Sakka, J. Am. Ceram. Soc. 76 (1993) 2486–2490.
[3] R.A.H. El-Mallawany, Tellurite Glasses Handbook, CRC Press, Boca Raton, 2001, p. 113.
[4] H. Nasu, O. Matsushita, K. Kamiya, H. Kobayashi, K. Kubodera, J. Non-Cryst. Solids 124 (1990) 275–277.
[5] Y. Chen, Q. Nie, T. Xu, S. Dai, X. Wang, X. Shen, J. Non-Cryst. Solids 354 (2008) 3468–3472.
[6] I. Kabalci, G. Özen, M.L. Öveçoğlu, A. Sennaroğlu, J. Alloys Compd. 419 (2006) 294–298.
[7] M.A.P. Silva, Y. Messaddeq, S.J.L. Ribeiro, M. Poulain, F. Villain, V. Briois, J. Phys. Chem. Solids 62 (2001) 1055–1060.
[8] S. Blanchandin, P. Thomas, P. Marchet, B. Frit, A. Chagraoui, J. Mater. Sci. 34 (1999) 4285–4292.
[9] S. Blanchandin, P. Thomas, P. Marchet, J.C. Champarnaud-Mesjard, B. Frit, J. Mater. Chem. 9 (1999) 1785–1788.
[10] J.C. Champarnaud-Mesjard, S. Blanchandin, P. Thomas, A. Mirgorodsky, T. Merle-Mejean, B. Frit, J. Phys. Chem. Solids 61 (2000) 1499–1507.
[11] S. Blanchandin, P. Thomas, P. Marchet, J.C. Champarnaud-Mesjard, B. Frit, J. Alloys Compd. 34 (2002) 206–212.
[12] A. Chagraoui, A. Chakib, A. Mandil, A. Tairi, Z. Ramzi, S. Benmokhtar, Scr. Mater. 56 (2007) 93–96.
[13] M. El-Hagary, M. Emam-Ismail, E.R. Shaaban, I. Shaltout, J. Alloys Compd. 485 (2009) 519–523.
[14] C. Zhao, G.F. Yang, Q.Y. Zhang, Z.H. Jiang, J. Alloys Compd. 461 (2008) 617–622.
[15] J.C. Sabadel, P. Armand, F. Terki, J. Pelous, D. Cachau-Herreillat, E. Philippot, J. Phys. Chem. Solids 61 (2000) 1745–1750.
[16] A. Chagraoui, Z. Ramzi, A. Tairi, A. Mandil, M. Talibouridah, K. Ajebli, Y. Abboud, J. Mat. Proc. Technol. 209 (2009) 3111–3116.
[17] R.D. Shannon, C.T. Prewitt, Acta Cryst. B25 (1969) 925–945.
[18] L.D. Pye, H.J. Stevens, W.C. Lacourse, Phys. Non-Crystalline Solids, Taylor and Francis, 1992, p. 281.
[19] Y.S. Low, H.A.A. Sidek, S.P. Chow, H.B. Senin, S.A. Halim, J. Fiz., UTM 6 (1999) 1.
[20] M. Dimitrova-Pankova, Y. Dimitriev, M. Arnaudov, V. Dimitrov, Phys. Chem. Glasses 30 (6) (1989) 260–263.
[21] T. Sekiya, N. Mochida, A. Ohtsuka, M. Tonokawa, Nippon Seramikkusu Kyokai Gakujutsu Ronbunshi, J. Ceram. Soc. Jpn. 97 (12) (1989) 1435–1440.
[22] O. Noguera, T. Merle-Méjean, A.P. Mirgorodsky, M.B. Smirnov, P. Thomas, J.C. Champarnaud-Mesjard, J. Non-Cryst. Solids 330 (2003) 50–60.
[23] Y. Dimitriev, Chim. Chronica, New Series 23 (1994) 361–366.
[24] M. Arnaudov, V. Dimitrov, Y. Dimitriev, L. Markova, Mater. Res. Bull. 17 (1982) 1121–1129.
[25] Q.T. Sekiya, N. Mochida, A. Ohtsuka, M. Tonokawa, J. Ceram. Soc. Jpn. 97 (1989) 1435–1440.
[26] S.T. Sekiya, N. Mochida, A. Ohtsuka, M. Tonokawa, J. Non-Cryst. Solids 144 (1992) 128–144.
[27] B.V.R. Chowdari, P. Pramoda Kumari, Mater. Res. Bull. 34 (2) (1999) 327–342.
[28] A. Boultif, D.J. Louer, Crystallogr. Appl. 24 (1991) 987–993.
[29] T. Kikuchi, T. Hatano, S. Horiuchi, J. Mater. Sci. Lett. 9 (1990) 580–582.
[30] J.C. Champarnaud-Mesjard, B. Frit, A. Chagraoui, A. Tairi, J. Solid State Chem. 127 (1996) 248–255.
[31] I. Nishantha, Thesis, M.A. The Ohio State University (2008).